

# Induced pluripotent stem cell-derived enteric neural crest cells repopulate human aganglionic tissue-engineered intestine to form key components of the enteric nervous system

David F Chang<sup>1\*</sup>, Samuel M Zuber<sup>1\*</sup>, Elizabeth A Gilliam<sup>1</sup>, Laura-Marie A Nucho<sup>1</sup>, Gabriel Levin<sup>1</sup>, Fengnan Wang<sup>1</sup>, Anthony I Squillaro<sup>1</sup>, Sha Huang<sup>2,3</sup>, Jason R Spence<sup>2,3,4</sup> and Tracy C Grikscheit<sup>1,5,6</sup>

## Abstract

Models for enteric neuropathies, in which intestinal nerves are absent or injured, are required to evaluate possible cell therapies. However, existing options, including transgenic mice, are variable and fragile. Here immunocompromised mice were implanted with human pluripotent stem cell-derived tissue-engineered small intestine 10 weeks prior to a second survival surgery in which enteric nervous system precursor cells, or saline controls, were injected into the human intestinal organoid-derived tissue-engineered small intestine and analyzed 4 weeks later. Human intestinal organoid-derived tissue-engineered small intestine implants injected with saline as controls illustrated formation of intestinal epithelium and mesenchyme without an enteric nervous system. Second surgical introduction of human pluripotent stem cell-generated enteric nervous system precursors into developing human intestinal organoid-derived tissue-engineered small intestine implants resulted in proliferative migratory neuronal and glial cells, including multiple neuronal subtypes, and demonstrated function in contractility assays.

## Keywords

Tissue-engineered small intestine, human intestinal organoids, enteric nervous system, Hirschsprung disease

Received: 28 August 2019; accepted: 18 January 2020

## Introduction

The enteric nervous system (ENS) regulates motility which can change absorption, microbial content, and function of the intestine, and lack or loss is morbid. This is termed enteric neuropathy, and results in obstruction, infection, and sometimes death. The most commonly encountered enteric neuropathy, affecting approximately 1 in 5000 neonates,<sup>1,2</sup> is Hirschsprung disease (HD). HD is caused by the failure of complete migration of the ENS into the distal intestine during fetal development, resulting in aganglionic, and therefore non-functional, intestine of varying lengths.

HD is not the only enteric neuropathy. In the stomach, gastroparesis is a frequent complication of diabetes,<sup>3</sup> some drugs, and neurodevelopmental disorders. Esophageal enteric neuropathy, or achalasia, is associated with the loss of innervation of the lower esophageal sphincter,<sup>4</sup> whether

<sup>1</sup>Developmental Biology and Regenerative Medicine Program, The Saban Research Institute, Children's Hospital Los Angeles, Los Angeles, CA, USA

<sup>2</sup>Department of Internal Medicine, Medical School, University of Michigan, Ann Arbor, MI, USA

<sup>3</sup>Department of Cell & Developmental Biology, Medical School, University of Michigan, Ann Arbor, MI, USA

<sup>4</sup>Program of Cellular & Molecular Biology, Medical School, University of Michigan, Ann Arbor, MI, USA

<sup>5</sup>Department of Surgery, Division of Pediatric Surgery, Children's Hospital Los Angeles, Los Angeles, CA, USA

<sup>6</sup>Keck Medical School, University of Southern California, Los Angeles, CA, USA

\*Shared first authorship.

## Corresponding author:

Tracy C Grikscheit, Developmental Biology and Regenerative Medicine Program, The Saban Research Institute, Children's Hospital Los Angeles, 4650 Sunset Blvd., Mailstop 100, Los Angeles, CA 90027, USA. Email: tgrikscheit@chla.usc.edu



idiopathic or due to parasitic infection. Enteric neuropathies also affect large numbers of patients via slow transit constipation, anal incontinence, and chronic intestinal pseudo-obstruction.<sup>5</sup>

The ENS has been styled “the second brain,” because the number of neurons within the ENS exceeds that of the spinal cord.<sup>6</sup> The ENS functions autonomously for control and modulation of intestinal motility, secretion, vasomotor function, and afferent sensing of stretch and luminal contents.<sup>7–9</sup> Now many of the tremendously diverse components of the ENS may be generated from both adult stem cells and human pluripotent stem cells (hPSCs).<sup>10–13</sup> Neurospheres, or adult stem/progenitor cells that will differentiate into various ENS components, may be derived from multiple intestinal regions and are well covered in the literature<sup>13</sup> but not discussed further here.

Vagally specified enteric neural crest cells (ENCCs) have been generated by multiple groups from hPSCs, with further successful *in vivo* differentiation into the markedly diverse cell types of the ENS.<sup>11,12,14</sup> These ENCCs are produced from variations of protocols initially developed to derive central and peripheral nerve cell lineages from hPSCs.<sup>15–18</sup> Changes in the timing of exposure to retinoic acid appear to be important to derive a more pure population of ENCCs.<sup>11,12,14</sup> A combined implant composed of ENCCs and hPSC-derived tissue-engineered small intestine (TESI) will demonstrate functional contractility.<sup>11</sup> Although it can be useful to evaluate these cells in native intestine with an intact ENS, this does not fully reproduce the clinical scenario of repopulating aganglionic intestine which is the ultimate goal of ENCC-based cell therapies. In order to test ENCC differentiation into ganglia and key neuronal subtypes and to assess cell proliferation and migratory capacity, it is necessary to evaluate ENCCs *in vivo*, in models that lack all of the components of the ENS.

Animal models that lack the ENS in some portion of the intestine are fragile and variable. The most commonly studied mouse models for HD include transgenic alterations of endothelin receptor type B (*Ednrb*). *Ednrb* models can be quite variable, with widely different amounts of intestine affected, even in littermates, which may cloud *in vivo* results and render rescue effects unknown.<sup>19</sup> Conversely, the variability can be so severe that the newborn mouse cannot survive. In one *Ednrb* model (B6.129S7-*Ednrb*<sup>tm1Ywa/Fryk</sup>)<sup>20</sup> thought to be less variable, although there are reported survivors of neonatal surgery, in our hands, the addition of immunosuppression in order to study implanted human cells, resulted in no short-term survivors. Therefore, in order to study the capacity of ENCC-derived components of the ENS in a survivable *in vivo* model, we sought to identify a more robust and reproducible method of administering donor cells to existing aganglionic intestinal tissue.

We and others have previously co-implanted ENCCs with human intestinal organoids (HIOs).<sup>11,14</sup> HIOs are produced *in vitro* by the differentiation of hPSCs into all of the components of the small intestine, and they always exclude any components of the ENS.<sup>10,21</sup> When HIOs and ENCCs are implanted in combination in one step, ENS components derived from ENCCs were identified in the form of submucosal and myenteric ganglia, as well as numerous subclasses of neurons. There were neuroepithelial connections to enteroendocrine cells.<sup>11</sup> However, this differs from the expected clinical scenario in human patients who will present with aganglionic intestinal tissue requiring therapy. Therefore, in order to investigate the capacity of ENCCs to migrate within aganglionic intestine, we hypothesized that staged survival surgeries, first developing aganglionic intestinal tissue (HIO-TESI), followed 10 weeks later by repeat survival surgery implanting the HIO-TESI with bioluminescent-tagged ENCCs, might allow *in vivo* tracking of the ENCCs in a more robust and reproducible model. Repeat survival laparotomies to add new cell types to growing engineered tissues had not previously been performed to our knowledge, but in this case were well tolerated. Both donor cell populations exhibited growth and differentiation, with functional contractility in a small sample, indicating the possible future value of a sequential HIO-TESI-ENCC model to evaluate and perfect cell therapies for enteric neuropathies.

## Methods

### Animal care

Non-obese diabetic/severe combined immunodeficient gamma mice (NOD/SCID, Jackson Labs, Cat 005557) were housed in sterile cages with sterile food and water with set day–night cycles in keeping with the National Institutes of Health’s Guide for the Care and Use of Laboratory Animals (2011). All protocols involving animals were approved by the Children’s Hospital of Los Angeles (CHLA) Institutional Animal Use and Care Committee (IACUC, Approval #215).

### HIO and ENCC generation

HIOs derived from H9 hPSCs (WiCell) to day 28–35 of age were generated as previously described.<sup>21</sup> To generate ENCCs, LiPSC-GR1.1 (Lonza)<sup>22</sup> completed a 15-day directed differentiation protocol as previously published.<sup>11,12</sup> Briefly, ENCCs were generated up to day 11 as described.<sup>11</sup> On day 11, adherent ENCCs were lifted and aggregated into three-dimensional (3D) spheroids in ultra-low attachment plates and cultured in neurobasal medium supplemented with N2/B7 containing 3 mM CHIR99021 and 1 nM FGF2 for additional 4 days. Cell samples were collected on day 0 (pre-differentiation) and day 15 (post-differentiation) for

immunostaining and flow analysis (see below). Prior to implantation, cells were labeled with indocyanine green (ICG) fluorescent dye (see below) and counted with a manual hemocytometer. Derivation of HIOs was approved by the institutional review board (IRB) at Cincinnati Children's Hospital Medical Center. Derivation of ENCCs was approved by the University of Southern California and Children's Hospital Los Angeles Stem Cell Research Oversight committee.

### Flow cytometry

Staining buffer consisted of 1X DPBS (Dulbecco's phosphate-buffered saline), without calcium and magnesium (VWR, Cat 21-031-CV), 5% FBS (Thermo Fisher, Cat 26140079), and 0.1% sodium azide. Antibodies CD271-PE (P75<sup>NTR</sup>) (Miltenyi Biotech, Cat 130-098-111), CD57-APC (HNK1) (Miltenyi Biotech, Cat 130-092-141), Mouse IgG1 Isotype control-PE (Miltenyi Biotech, Cat 130-092-212), and Mouse IgM Isotype control-APC (Miltenyi Biotech, Cat 130-093-176) were diluted in prepared staining buffer as described in manufacturer's instructions. CD271 and CD57 were combined in one solution and isotype controls in a second solution to allow for dual staining. A 50 µg/mL DAPI solution was diluted 1:500 in staining buffer. Cells were collected and washed with 1X DPBS and dissociated with Accutase (Innovative Cell Technologies, Cat AT-104) at 37°C for 3 min; 1.5× the volume of cold NB/N2 media was added to deactivate the Accutase. A 20 µL sample was taken to count the cells with the Invitrogen Countess (Invitrogen, Cat C10227). Based on these counts, the remaining cells were centrifuged at 300 g for 3 min at 4°C, and the supernatant aspirated. The cells were then stained in 100 µL of antibody solution for 60 min. They were again centrifuged under the same settings. The cells were washed with staining buffer, resuspended in 500 µL of staining buffer with DAPI, and flow data were created by a BD LSR II analytic cytometer.

### ICG labeling

Modified from a previously described method,<sup>23</sup> ICG fluorescent dye (Santa Cruz Biotech, Cat sc-217845a) was reconstituted in DMSO and added to day 15 ENCC differentiation media to achieve a concentration of 2 mg/mL. ENCCs used for implantation were incubated in the solution for 1 h at 37°C, away from light. Cells were then washed and resuspended in the day 15 ENCC differentiation media and counted with a manual hemocytometer.

### Surgical procedures

Mice received isoflurane anesthesia for all surgeries. The ventral fur of the mouse was removed either with a clipper

or a depilatory cream (Nair, Church & Dwight). Operated mice received Ketofen (5 mg/kg, Zoetis) subcutaneously for pain control and were allowed to recover in sterile post-operative cages with sterile water supplemented with Enroflox antibiotic (0.5 mg/mL, Norbrook Laboratories Limited). The initial surgery consisted of a midline laparotomy incision with evisceration of the greater omentum which was spread out as a thin sheet. A hollow cylindrical biodegradable scaffold seeded with 10–12 HIOs in 60 µL of intestinal growth media<sup>21</sup> was placed into the center of the omentum which was then carefully folded to completely envelop the scaffold. A single stitch was placed to keep the omentum and scaffold in place relative to each other. The construct was then returned to the abdomen and the laparotomy was closed. A video of our scaffold preparation and implantation process is available on JoVE.<sup>24</sup> Implanted HIOs were allowed to grow into TESI for 10 weeks. One week prior to the second surgery, the mice's diet was switched to alfalfa-free chow (Teklad Global 16% Protein Rodent Diet, Envigo, Cat 2916.15) to avoid abdominal autofluorescence that might interfere with subsequent *in vivo* imaging system (IVIS) imaging. During the second surgery, the previous midline laparotomies were re-opened. If no TESI construct had grown, the mice were excluded and humanely euthanized. If TESI growth was identified, either 100 µL of normal saline or  $1.0 \times 10^5$  ICG-labeled ENCCs in D15 media were injected into the TESI. The TESI was then returned to the abdomen and the laparotomy was closed. The mice were imaged twice weekly for remaining ICG signal (described below). Four weeks post ENCC implantation (second surgery), mice were imaged prior to TESI extraction. TESI explants were either again imaged with IVIS for remaining signal (n=5) or placed in a 37°C 5% CO<sub>2</sub> incubator for the contractility assay (n=4; described below). For the ICG-labeling experiment, mice were implanted with HIOs (n=9). Five mice successfully grew TESI, and were injected with either saline as controls (n=1) or D15 ENCC (n=4). For the contractility experiment, a total of five mice were implanted with HIOs. Four mice successfully grew TESI, and were injected with either saline (n=1) or D15 ENCC (n=3).

### IVIS imaging

Noninvasive bioluminescence imaging was performed with an IVIS Spectrum 200 (Perkin-Elmer). After saline or ICG-tagged ENCC injection, mice were imaged on post-operative days 3, 7, 10, 14, 17, 21, 24, 28, and 31 under isoflurane anesthesia. During imaging sessions, a depilatory cream (Nair, Church & Dwight) was applied on the mouse abdomen near the region of interest (ROI) as needed. On day 31, we also imaged TESI explants which were washed with PBS (phosphate-buffered saline), bisected, and imaged. Fluorescence signals within the ROI

**Table 1.** Summary of antibodies used.

| Antibody                         | Primary or secondary | Species | Dilution | Supplier and Cat #      |
|----------------------------------|----------------------|---------|----------|-------------------------|
| 5-HT (Serotonin)                 | Primary              | Mouse   | 1:200    | ThermoFisher #MA5-12111 |
| CALB (Calbindin)                 | Primary              | Rabbit  | 1:200    | Millipore #AB1776       |
| CHAT (Choline Acetyltransferase) | Primary              | Rabbit  | 1:200    | Bioss #BS-0042R         |
| CHGA (Chromogranin A)            | Primary              | Rabbit  | 1:200    | Abcam #ab15160          |
| CKit (c-Kit)                     | Primary              | Rabbit  | 1:200    | Abcam #ab32363          |
| ECAD (E-Cadherin)                | Primary              | Mouse   | 1:200    | BD Bioscience #610181   |
| CD57-APC (HNK1)                  | Primary              | Mouse   | 1:50     | Miltenyi #130118665     |
| LAMIN (Lamin A + C)              | Primary              | Rabbit  | 1:200    | Abcam #ab108595         |
| LYSO (Lysozyme)                  | Primary              | Rabbit  | 1:200    | Dako #A0099             |
| MUC2 (Mucin2)                    | Primary              | Rabbit  | 1:200    | Santa Cruz #SC-15334    |
| NOS1 (nNOS)                      | Primary              | Rabbit  | 1:200    | Santa Cruz #SC-648      |
| OCT4                             | Primary              | Rabbit  | 1:200    | Abcam #ab109183         |
| CD271-PE (P75 <sup>NTR</sup> )   | Primary              | Mouse   | 1:50     | Miltenyi #130113983     |
| PCNA                             | Primary              | Mouse   | 1:200    | Abcam #ab29             |
| PGP 9.5                          | Primary              | Rabbit  | 1:200    | Dako #Z5116             |
| Mouse IgG1-PE                    | Primary              | Mouse   | 1:50     | Miltenyi #130113762     |
| Mouse IgM-APC                    | Primary              | Mouse   | 1:50     | Miltenyi #130099085     |
| Alexa Fluor 488                  | Secondary            | Donkey  | 1:200    | ThermoFisher #A-21202   |
| Donkey anti-Mouse IgG (H + L)    |                      |         |          |                         |
| Alexa Fluor 546                  | Secondary            | Donkey  | 1:200    | ThermoFisher #A-10040   |
| Donkey anti-Rabbit IgG (H + L)   |                      |         |          |                         |

For immunostaining, antibodies were diluted in Universal Blocking Solution with 2% donkey serum. Universal Blocking Solution consists of 1% BSA, 0.1% cold fish skin gelatin, and 0.5% Triton X-100 in PBS. For flow cytometry, antibodies were diluted in staining solution consists of 5% FBS in 1 × DPBS. BSA: bovine serum albumin; PBS: phosphate-buffered saline; DPBS: Dulbecco's phosphate-buffered saline.

were measured in radiant efficiency (p/s/cm<sup>2</sup>/sr)/(μW/cm<sup>2</sup>) and analyzed in the Living Image 4.5.5 software (Perkin-Elmer). Graphs of the ROI area were plotted against time courses for each mouse in Microsoft Excel.

### Immunofluorescence staining analysis

Cells (D0 hPSC and D15 ENCC) were harvested, embedded into 3% low melting agarose, fixed in 10% formalin overnight, then embedded in paraffin. TESI were extracted, fixed in 10% formalin overnight, then embedded in paraffin; 5 μm sections were cut and used for immunofluorescence staining. Slides were deparaffinized and rehydrated. Antigen retrieval was performed with 1 M Tris-HCl (pH=8.6) (Bioland Scientific, Cat Tris86) heated in a pressure cooker. Slides were washed in PBS with 0.1% Tween (Sigma Aldrich, Cat P1379-1L), blocked and permeabilized in Universal Blocking Solution made from 1% BSA (Sigma Aldrich, Cat A7906-50G), 0.1% cold fish skin gelatin (Sigma Aldrich, G7041-100G), and 0.5% Triton X-100 (Sigma Aldrich, Cat T8787-250ML) in PBS. Primary antibodies (Table 1) were applied at 1:200 dilution for 2h at room temperature. Secondary antibodies (Table 1) were applied at 1:200 dilution for 1h at room temperature. Slides were preserved with VECTASHIELD Mounting Medium with DAPI (Vector Labs, Cat H1200)

and imaged on a Leica DMI6000 B inverted fluorescence microscope.

### Contractility assay

Mechanical contraction of TESI was studied as previously described.<sup>11</sup> Time-lapse video microscopy was captured with a Leica MZ12.5 stereoscope equipped with a Leica MC179 HD digital camera. Explanted TESIs were placed in clear FluoroBrite DMEM media (ThermoFisher, Cat A1896701), incubated for 30 min at 37°C, followed by initial evaluation for spontaneous contractility. TESI explants that showed signs of movement were flushed intraluminally with FluoroBrite DMEM to remove any previously produced mucus and placed back in the incubator for 30 min and then filmed for 3 min prior to chemical treatments (Movies S1–S4 in supplemental material). Afterward, the contracting samples were injected intraluminally with methylene blue (MB, Acros, Cat 122965-43-9) diluted in FluoroBrite DMEM (50 μM), and whole explants were immersed in MB solution for 3.5 h under a 40 W lamp at room temperature to cause selective lesioning of enteric pacemaker cells, the interstitial cells of Cajal (ICC). The TESI were again incubated for 30 min, followed by video imaging for at least 3 min (Movies S5–S8 in supplemental material). TESI that continued to contract were injected intraluminally and immersed in a

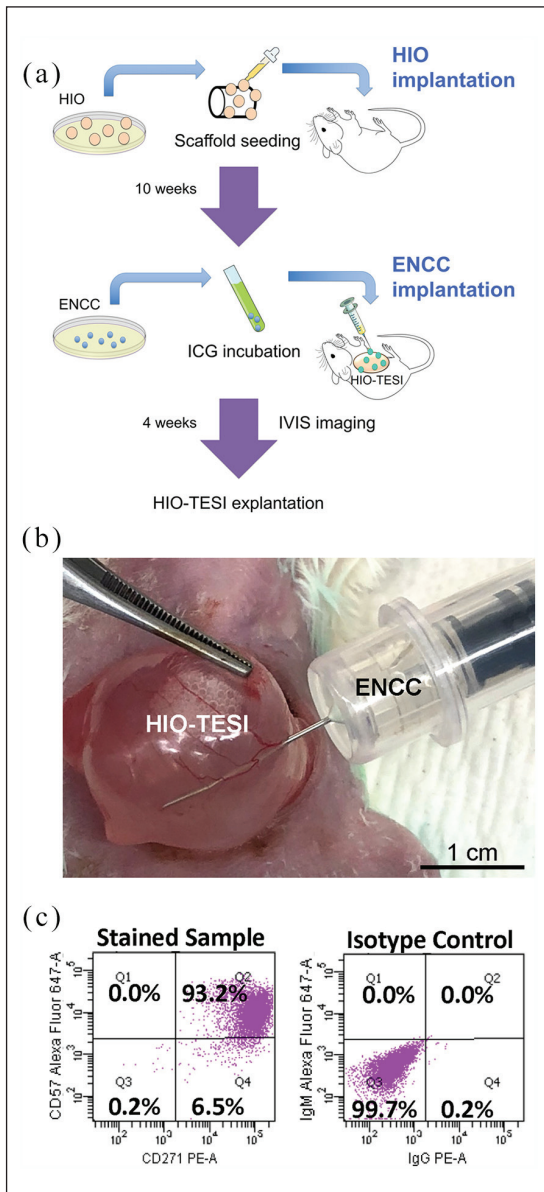


**Figure 1.** Sequential survival laparotomies to successively combine components of tissue-engineered small intestine: (a) Schematic illustration of the “double-surgery” procedure, followed by IVIS bioluminescence imaging and explantation. (b) Injection of ICG-tagged ENCCs into HIO-TESI during second survival operation. (c) Flow cytometry of ENCCs for CD271 (P75<sup>NTR</sup>) and CD57 (HNK1) at day 15. Isotype control antibodies were applied. HIO: human intestinal organoid; ENCC: enteric neural crest cell; ICG: indocyanine green dye; HIO-TESI: tissue-engineered small intestine derived from human intestinal organoids; IVIS: in vivo imaging system.

neurotoxin, tetrodotoxin (Abcam, Cat ab120055), diluted in FluoroBrite DMEM (10  $\mu$ M) for 4 h in 37°C, then filmed (Movies S9–S11 in supplemental material). Videos were filmed for at least 5 min and then post-processed to 20 $\times$  speed in iMovie v10.1.10.

## Results

In contrast to previous work in which ENCCs and HIOs were co-implanted, in this study we performed sequential surgeries (Figure 1(a)) to administer different hPSC cell types to more closely approximate the clinical scenario that we are likely to encounter in patients with enteric neuropathies. Ten weeks prior to adding ENCCs, we seeded 10–12 HIOs on biodegradable scaffolds and implanted them into the greater omentum of immunocompromised NOD/SCID mice to develop TESI. Then in a second survival surgery, saline (control) or  $1.0 \times 10^5$  hPSC-derived ENCCs, labeled with ICG dye, were injected into the mature TESI (Figure 1(b)) 4 weeks prior to eventual harvest. ICG is a fluorescent dye that is FDA-approved for medical diagnostics. Presence of ICG-tagged signal was monitored with IVIS imaging every 3 or 4 days post injection (Figure 2(a) and (b)). Persistent fluorescence was detected in one mouse and the corresponding implant (M09, Figure 2(a) and 2(b)) until the time of explantation, 31 days post injection (Figure 2(c)).

In order to verify that the implanted ENCCs were successfully generated from hPSCs after 15 days in culture, we performed flow cytometry and identified more than 90% double-positive cells for HNK1 (CD57) an P75<sup>NTR</sup> (CD271) markers<sup>25</sup> (Figure 1(c)). Furthermore, immunostaining revealed the presence of neurons and glia. Compared to day 0 (D0) undifferentiated hPSCs, TUJ1-positive (Figure 3(a), (h), (i), and (j)) and PGP9.5-positive staining (Figure 3(k)) indicate the appearance of neurons by day 15 (D15) post-differentiation. Specific subtypes of neurons, however, are not identified at this time (CALB-, 3(h); CHAT-, 3(i); NOS1-, 3(j); 5-HT-, 3(k)). S100 $\beta$ -positive glial cells are also present in D15 hPSCs (Figure 3(b)). Although markers for mesenchymal cell lineage, CKIT (Figure 3(c)) and SMA (Figure 3(d)), are absent in differentiated neurospheres, a small percentage of cells in D15 hPSCs express epithelial marker ECAD (Figure 3(e), (f), and (g)). Nevertheless, specific epithelial cell lineage markers, MUC2 (Figure 3(e)), CHGA (Figure 3(f)), and LYSO (Figure 3(g)), are not detected. Noticeably, despite the fact that D15 ENCCs demonstrate proliferative capacity with a high level of PCNA expression (Figure 3(l)), pluripotency marker OCT4 is completely absent (Figure 3(m)), reducing concern for teratoma formation after engraftment. Human-specific staining against nuclear envelope protein LAMIN identifies human ENCCs after xenotransplantation (Figure 3(n)).

One month after the second surgery, in which ENCCs were delivered to the TESI, the HIO-TESI or HIO-ENCC-TESI were explanted to further characterize their cellular composition. Tissues were sectioned and stained with antibodies against TUJ1 for neurons (Figure 4(a) and (b)); S100 $\beta$  for glia (Figure 4(b)); CKIT (Figure 5(a)) and SMA (Figure 5(b)) for the mesenchymal

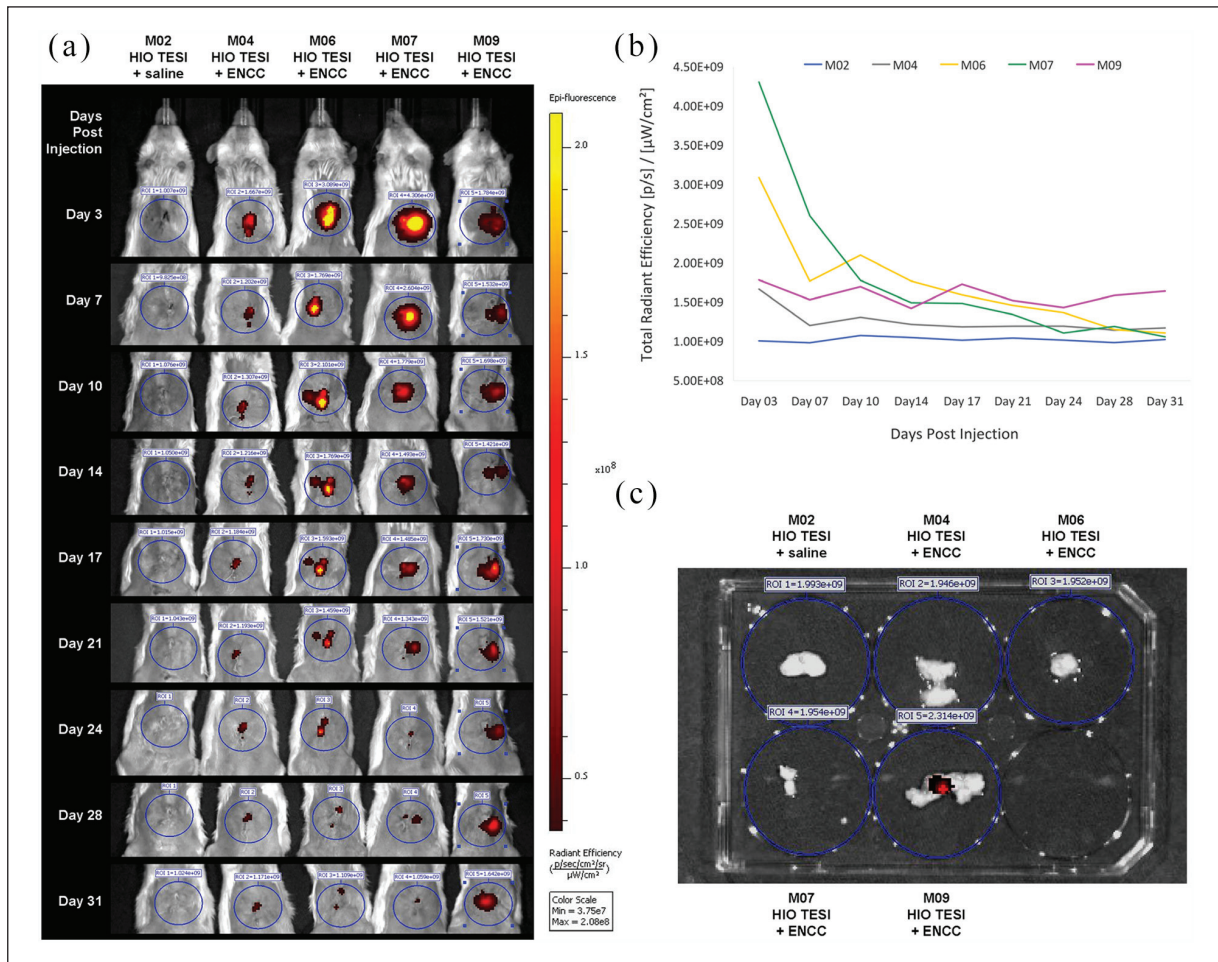


**Figure 2.** In vivo monitoring of fluorescent dye-tagged enteric neural crest cells: (a) Following injection of saline (control) or ICG-labeled ENCCs into HIO-TESI, immunocompromised mice with implants were followed twice weekly by IVIS imaging, up to 31 days, for photon emission around the region of interest (circled). The mice were imaged ventrally, with their abdominal area shaved, to avoid background signal from animal hair. The color bar indicates the signal intensity, with yellow and dark red representing the high and low bioluminescent signals, respectively. (b) Bioluminescence in five mice (M02, M04, M06, M07, M09) was monitored before TESI recovery on day 31. (c) TESI explants were bisected, washed, and imaged for residual fluorescence. ICG: indocyanine green dye; ENCC: enteric neural crest cell; HIO-TESI: tissue-engineered small intestine derived from human intestinal organoids; IVIS: in vivo imaging system.

component; and ECAD (Figure 5(c), (d), and (e)), MUC2 (Figure 5(c)), CHGA (Figure 5(d)), and LYSO (Figure 5(e)), for the epithelial component. Compared to native human ileum, HIO-TESI with ENCC injection, but not the saline control injection, displayed neuronal and glial cells, forming ganglion-like clusters (arrows, Figure 4(a) and (b)) in close proximity to the epithelium (e) and within the muscle layer of TESI (arrowheads). This corresponds to two known locations in native intestine (Meissner's and Auerbach's plexus). In HIO-TESI with ENCC injection, TUJ1-positive cells co-stained with human-specific antibody against LAMIN (Figure 4(a)), confirming that the re-populated neurons are from the donor ENCCs. We also detected intrinsic enteric pacemakers known as ICC (CKIT+, Figure 5(a)) and smooth muscle cells (SMA+, Figure 5(b)). Both HIO-TESI with

ENCCs and HIO-TESI with mock saline injection developed villus-like epithelium (ECAD+, Figure 5(c)–(e)), consisting of various types of enterocytes, including goblet cells (MUC2+, Figure 5(c)), enteroendocrine cells (CHGA+, Figure 5(a)) and Paneth cells (LYSO+, Figure 5(e)). The HIO-TESI epithelium contains highly proliferative cells (PCNA+, Figure 5(f)), but lacks OCT4 expression throughout (Figure 5(f)).

In order to further delineate the composition of engrafted neurons in HIO-ENCC-TESI, we tested TUJ1-positive or PGP9.5-positive ganglia with an array of antibodies against different neuronal subtypes, including calbindin (CALB, Figure 6(a)), choline acetyltransferase (CHAT, Figure 6(b)), neuronal nitric oxide synthase (NOS1, Figure 6(c)), and serotonin (5-HT, Figure 6(d)). As shown, calbindin immunoreactive type III sensory neurons (CALB,

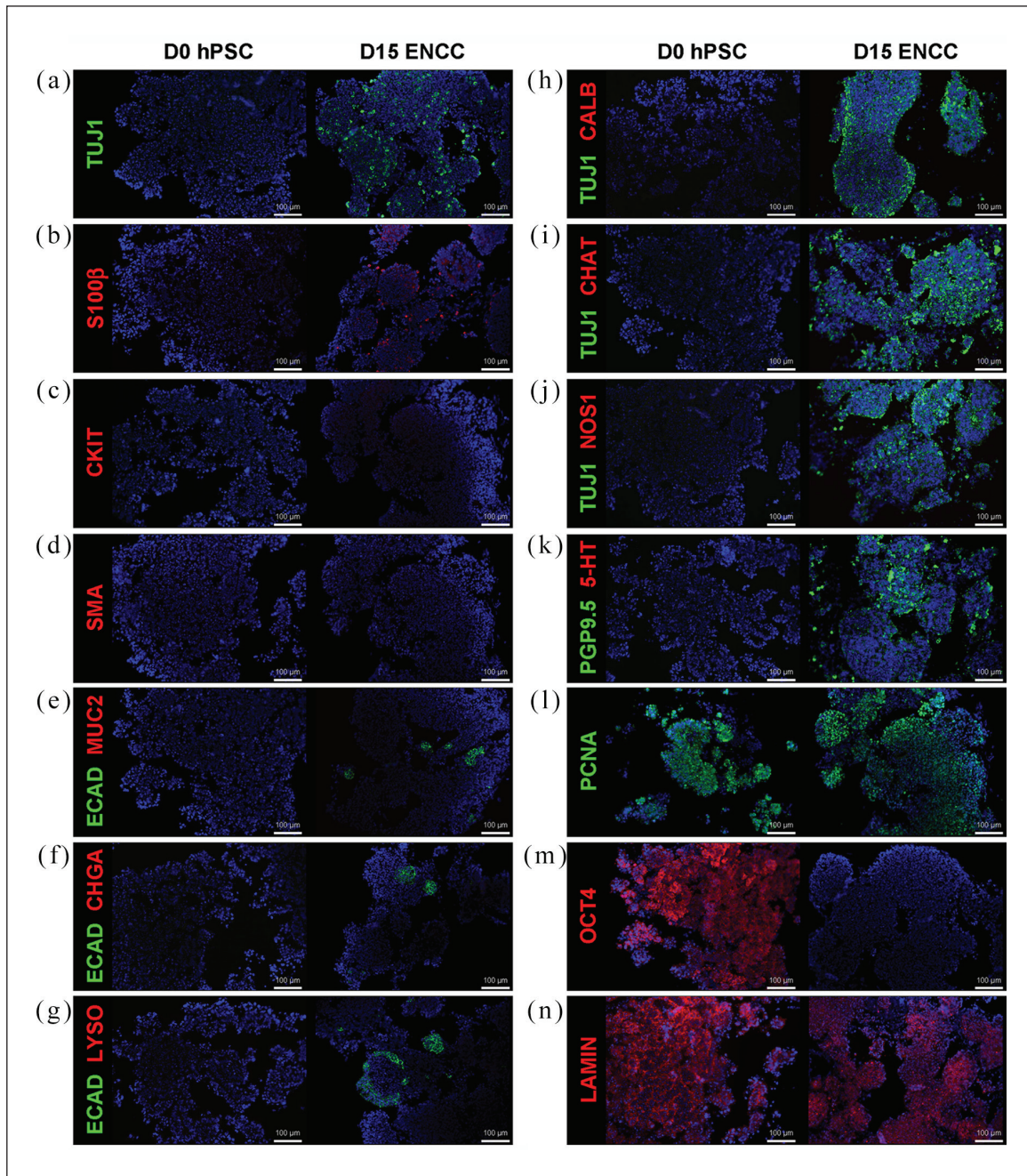


**Figure 3.** In vitro differentiation of human pluripotent stem cells into enteric neural crest cells. Detailed immunofluorescence staining analysis confirms successful derivation of ENCCs from hPSCs. Neurons (TUJ1<sup>+</sup>, a, h, i, j, and PGP9.5<sup>+</sup>, k) and glia (S100β<sup>+</sup>, b) appear in differentiated D15 ENCCs, but not in pre-differentiation D0 hPSCs. Epithelial marker ECAD is expressed in a small population of D15 neurospheres, but no specific epithelial cell lineage is identified in ECAD<sup>+</sup> cells (MUC2<sup>-</sup>, e; CHGA<sup>-</sup>, f; LYSO<sup>-</sup>, g). Specific subtypes of neurons are not detected in D15 cells (CALB<sup>-</sup>, h; CHAT<sup>-</sup>, i, NOS1<sup>-</sup>, j; 5-HT<sup>-</sup>, k). Markers for mesenchymal cell lineage, CKIT (c) and SMA (d), are absent in ENCCs. Pluripotency marker OCT4 (m) is not expressed in D15 neurospheres. PCNA<sup>+</sup> indicates cell proliferation (l) and LAMIN<sup>+</sup> (n) marks the human origin of engraft cells. DAPI (blue) stains cell nuclei in all images. TUJ1: class III beta-tubulin; S100β: calcium binding protein B of the S100 family; CKIT: ICC-selective receptor tyrosine kinase; SMA: alpha-smooth muscle actin; ECAD: E-cadherin; MUC2: mucin 2; CHGA: chromogranin A; LYSO: lysozyme; CALB: calbindin; CHAT: choline acetyltransferase; NOS1: neuronal nitric oxide synthase; 5-HT: serotonin/5-hydroxytryptamine; PGP9.5: protein gene product 9.5; PCNA: proliferating cell nuclear antigen; OCT4: octamer-binding transcription factor 4; LAMIN: human-specific nuclear envelope protein lamin. D0: day 0 (pre-differentiation); D15: day 15 (post-differentiation); hPSC: human pluripotent stem cell; ENCC: enteric neural crest cell; ICC: interstitial cells of Cajal.

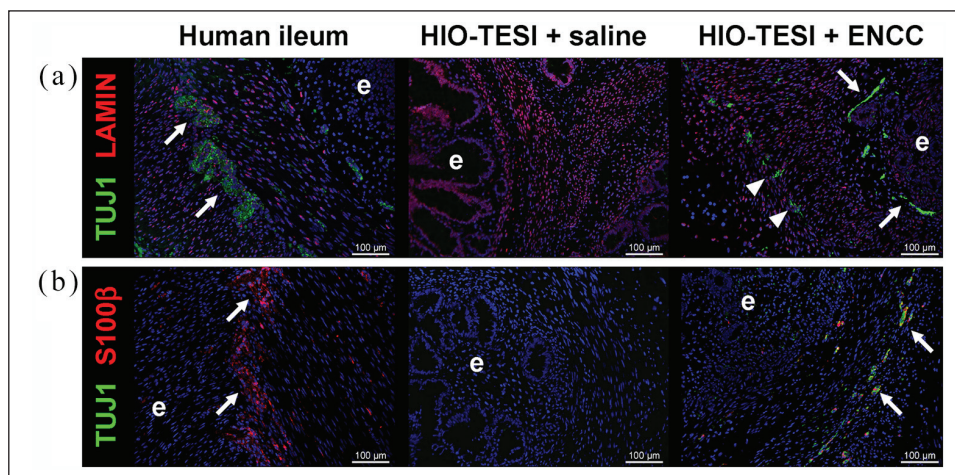


**Figure 4.** In vivo development of restored enteric nervous system in aganglionic tissue-engineered small intestine: Immunostaining analysis of HIO-TESI with control saline injection reveals a lack of enteric ganglia normally found in native adult human ileum (arrows, a and b). Addition of ENCCs derived from hPSCs (LAMIN+, a) in the second engraftment procedure reintroduces TUJ1+ neurons and S100β+ glia in ganglion-like clusters (arrows, a and b) near the epithelium (e). TUJ1+ cells are also observed in the muscle layers (arrowheads). DAPI stained cell nuclei in all images. TUJ1: class III beta-tubulin; LAMIN: human-specific nuclear envelope protein laminin; S100β: calcium binding protein B of the S100 family; hPSC: human pluripotent stem cell; ICC: interstitial cells of Cajal; HIO-TESI: tissue-engineered small intestine derived from human intestinal organoids.

Figure 6(a)),<sup>26</sup> excitatory neurons (CHAT, Figure 6(b)), inhibitory neurons (NOS1, Figure 6(c)), and descending interneurons (5-HT, Figure 6(d)) are identified.<sup>27</sup> This unique combination of neuronal subtypes recapitulates those found in native intestine. A table summarizes the immunostaining results reported in this study (Table 2).

In a pilot study of the function of these sequentially transplanted HIO-ENCC-TESI, explants of HIO-TESI with or without ENCCs exhibited spontaneous contraction and relaxation in vitro (Movies S1–S4 in supplemental material). But upon incubation with MB and light, which are known to cause selective lesioning of ICC,<sup>28</sup> contractility is notably blocked in the aganglionic control HIO-TESI (Movie S5 in supplemental material), but not inhibited in HIO-TESI supplemented with ENCCs (Movies S6–S8 in supplemental material). Only after subsequent treatment with potent neurotoxin tetrodotoxin (TTX) did two out of three HIO-ENCC-TESI completely abolish rhythmic motility (Movies S9–S11 in supplemental material). Since TTX selectively blocks the firing of action potentials in neurons, we reasoned that the persisting contractility in HIO-ENCC-TESI following MB treatment is independent of ICC, demonstrating functional restoration of engrafted ganglia. Interestingly, in the largest construct, contractility of one HIO-ENCC-TESI persisted despite MB and TTX treatment.

## Discussion

Because animal models for aganglionosis are variable, fragile, and may not recapitulate the human condition, we attempted to identify a more robust and reproducible

model in which to study the migration, maturation, and proliferation of precursor cells that form the ENS. Repeat survival surgery in humans is sometimes performed for sequential attempts to control tumor metastasis, evolving infections, incisional hernia, or chronic inflammatory states such as Crohn's disease, among other indications. However, repeated abdominal surgeries are known to convey increased risks including intestinal perforations from adhesiolysis, increased post-operative mortality, and wound healing problems.<sup>29</sup> These may be magnified in rodent surgery when post-operative care may be more limited. However, we had no deaths in our sequential surgery group despite waiting a total of 14 weeks for the growth of the constructs with multiple anesthetic administrations for survival surgery and identification of bioluminescent signal. The bioluminescent signal was identified from all sequentially implanted candidates after injection (Figures 1(a), (b), and 2(a)), allowing us to conclude that there was successful delivery. Despite the HIO-TESI having grown markedly (Figure 1(b)), an experienced surgeon may still inject ENCCs and return the growing TESI to the abdomen for a further 4 weeks after repeat laparotomy without complication. The injected ENCCs are then given time to proliferate, differentiate, and migrate within an already present tissue construct.

Optical imaging with ICG is FDA-approved for some human indications and can track cells of interest such as ES-derived cardiomyocytes for 48 h<sup>30</sup> or neurons in skin or spinal cord injury models in which its extinction time was recorded at 12–21 days.<sup>31</sup> We saw a marked diminution of signal over time, but in one explant could still identify ICG, presumably labeling the cells that were later identified, at

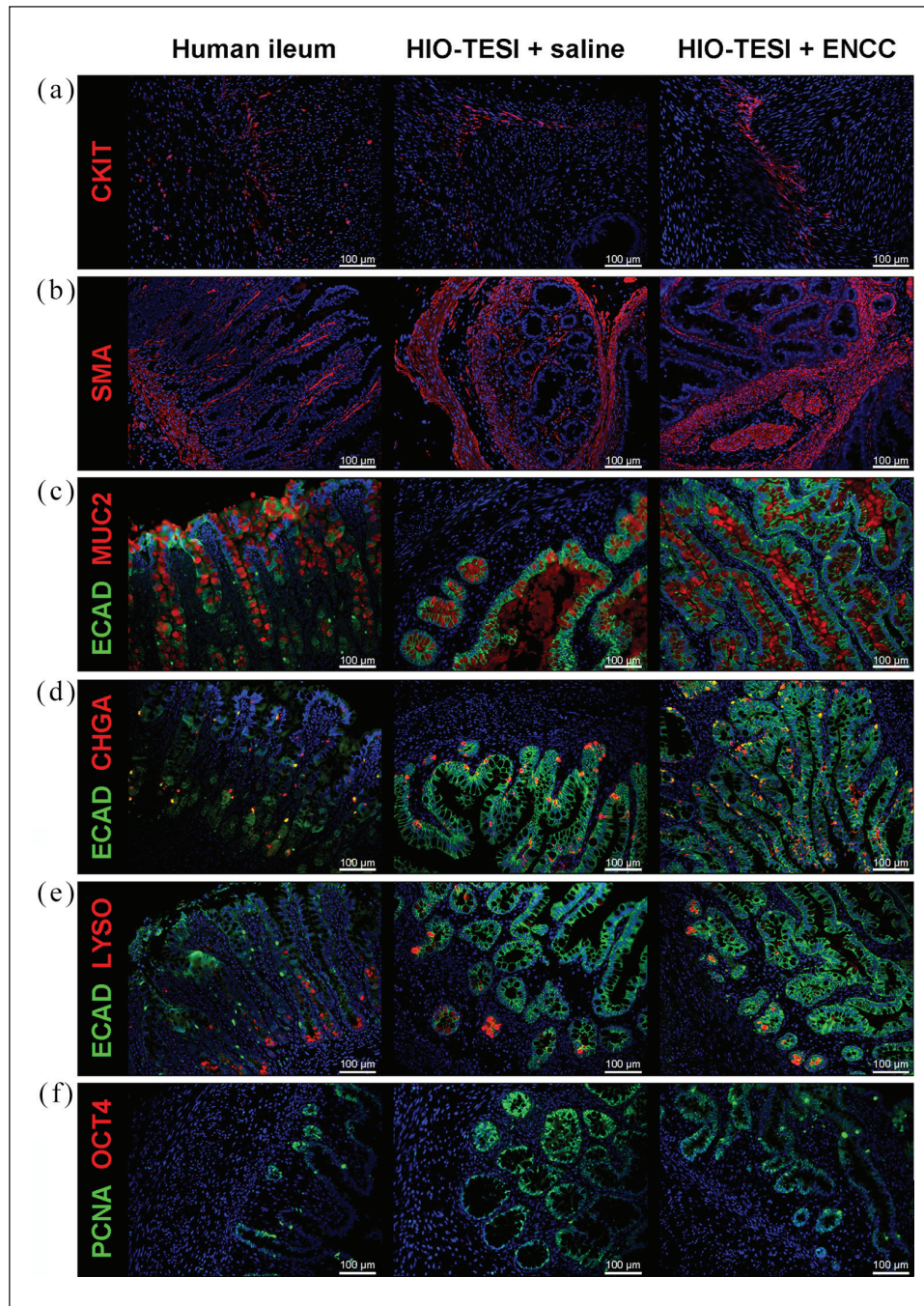


**Figure 5.** Human intestinal organoid–derived aganglionic tissue-engineered small intestine. Intestinal pacemaker cells ICC (CKIT+, a) and smooth muscle cells (SMA+, b) are identified in HIO-TESI with or without ENCC injection. Different cell types of epithelial lineage (ECAD+), including goblet cells (MUC2+, c), enteroendocrine cells (CHGA+, d), and Paneth cells (LYSO+, e), are present in HIO-TESI + saline and HIO-TESI + ENCC cysts. PCNA+ proliferating cells are located in the crypts and villus regions in the TESI (f). No OCT4 teratoma marker is observed (f). DAPI stained cell nuclei in all images. CKIT: ICC-selective receptor tyrosine kinase; SMA: alpha-smooth muscle actin; ECAD: E-cadherin; MUC2: mucin 2; CHGA: chromagranin A; LYSO: lysozyme; CALB: calbindin; CHAT: choline acetyltransferase; NOS1: neuronal nitric oxide synthase; 5-HT: serotonin/5-hydroxytryptamine; PGP9.5: protein gene product 9.5; PCNA: proliferating cell nuclear antigen; OCT4: octamer-binding transcription factor 4; hPSC: human pluripotent stem cell; ICC: interstitial cells of Cajal; HIO-TESI: tissue-engineered small intestine derived from human intestinal organoids.

31 days (Figure 2(a)). The combination of repeat survival surgery for sequential hPSC dosing and ICG cell tracking for longer time points may be helpful for future hPSC investigations in this and other models.

Assessing the HIO-ENCC-TESI compared to HIO-TESI alone, immunostaining identifies that transplantation of the ENCCs results in TUJ1-positive cells that are also LAMIN-positive. This confirms the human origin of these

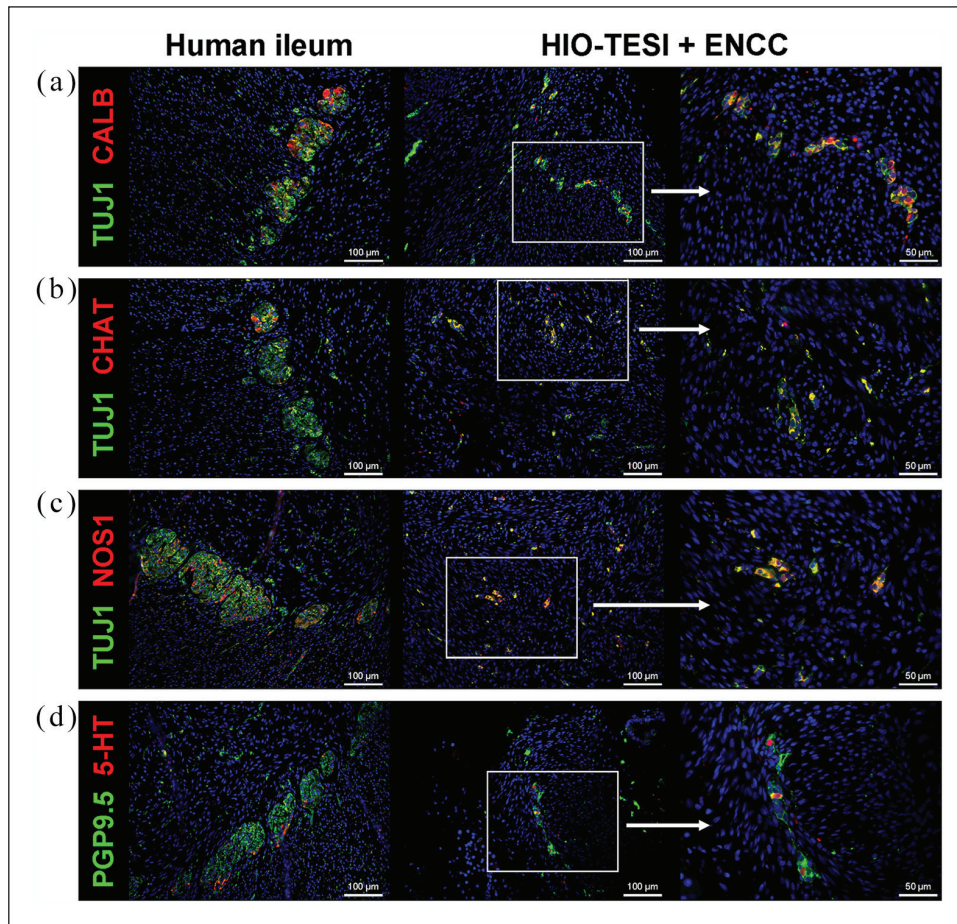


**Figure 6.** Diverse neuronal subtypes are present in re-populated ganglia. Immunofluorescence staining of HIO-TESI with ENCC injection identifies TUJ1+ or PGP9.5+ ganglia express markers for various subclasses of enteric neurons, including calbindin immunoreactive type III sensory neurons (CALB+, a), excitatory neurons (CHAT+, b), inhibitory neurons (NOS1, c), and descending interneurons (5-HT+, d). DAPI stains cell nuclei in all images. TUJ1: class III beta-tubulin; CALB: calbindin; CHAT: choline acetyltransferase; NOS1: neuronal nitric oxide synthase; 5-HT: serotonin/5-hydroxytryptamine; PGP9.5: protein gene product 9.5; HIO-TESI: tissue-engineered small intestine derived from human intestinal organoids.

**Table 2.** Summary of immunostaining performed in this report.

|                   | TUJ1 | S100 | CKIT | SMA | ECAD | MUC2 | CHGA | LYSO | CALB | CHAT | NOS1 | 5-HT | PCNA | OCT4 | LAMIN |
|-------------------|------|------|------|-----|------|------|------|------|------|------|------|------|------|------|-------|
| Human ileum       | +    | +    | +    | +   | +    | +    | +    | +    | +    | +    | +    | +    | +    | -    | +     |
| D0 hPSC           | -    | -    | -    | -   | -    | -    | -    | -    | -    | -    | -    | -    | +    | +    | +     |
| D15 hPSC (ENCC)   | +    | +    | -    | -   | +    | -    | -    | -    | -    | -    | -    | -    | +    | -    | +     |
| HIO-TESI + SALINE | -    | -    | +    | +   | +    | +    | +    | +    | -    | -    | -    | -    | +    | -    | +     |
| HIO-TESI + ENCC   | +    | +    | +    | +   | +    | +    | +    | +    | +    | +    | +    | +    | +    | -    | +     |

+: positive staining for the indicated antibody; -: negative staining for the indicated antibody. TUJ1: pan-neuronal class III beta-tubulin; S100 $\beta$ : glial-selective calcium binding protein B of the S100 family; CKIT: ICC-selective receptor tyrosine kinase; SMA: alpha-smooth muscle actin; ECAD: epithelial E-cadherin; MUC2: goblet cell-selective mucin 2; CHGA: enteroendocrine-selective chromogranin A; LYSO: Paneth cell-selective lysozyme; CALB: intrinsic sensory neuron-selective calbindin; CHAT: excitatory neuron-selective choline acetyltransferase; NOS1: inhibitory neuron-selective neuronal nitric oxide synthase; 5-HT: sensory neuron-selective serotonin/5-hydroxytryptamine; PGP9.5: pan-neuronal protein gene product 9.5; PCNA: proliferating cell nuclear antigen; OCT4: octamer-binding transcription factor 4; LAMIN: human-specific nuclear envelope protein lamin. hPSC: human pluripotent stem cell; D0: day 0 (pre-differentiation); D15: day 15 (post-differentiation); ENCC: enteric neural crest cell; HIO-TESI: tissue-engineered small intestine derived from human intestinal organoid; ICC: interstitial cells of Cajal.

neuronal clusters that are located subjacent to the epithelial layer that had formed over the first 10 weeks after implantation of the HIOs (Figure 4(a)). Furthermore, these ganglion-like clusters are also S100 $\beta$ -positive. As in previous studies in multiple labs,<sup>10,11,32</sup> HIO-TESI initially forms the expected differentiated epithelial cell types (Paneth, enteroendocrine, secretory cells) and mesenchymal cell types (smooth muscle with visible endothelium-lined networks of vascularization). Only the addition of ENCCs results in ganglia and neurons, with the neurons further specified as intrinsic sensory (calbindin), excitatory (CHAT), and descending interneurons (5-HT), with NOS1 also identified (Figure 5, Table 2). Yet, these differentiated cell types arose in vivo after the second survival surgery and are not identified prior to transplantation (Figure 3). The pluripotent donor cell, which is available as a cGMP-manufactured hPSCs<sup>22</sup> for possible future human applications retains pluripotent marker OCT4 at day 0 but this is absent prior to transplantation at day 15 (Figure 3). The absence of OCT4 is important for eventual release criteria of an ENCC cell product, which must not contain pluripotent cells that might result, at high enough cell numbers, in teratoma formation or the formation of unwanted cell types.

The TUJ1- and S100 $\beta$ -positive cells that are identified in the ENCCs just prior to transplantation are not organized into ganglia and are diffusely located in the donor ENCCs (Figure 3). Calbindin, CHAT, NOS1, and 5-HT are not present (data not shown) and are only generated subsequent to transplantation (Figure 6). This confirms that a true progenitor population is transplanted in the second procedure. The transplanted ENCCs do not contain intestinal epithelial or mesenchymal markers (Figure 3) although ECAD is noted in small populations. Because ECAD is a cell surface adhesion protein, we are not certain of the significance of detection of small amounts in vitro.

Initial study of the function of these sequentially transplanted HIO-ENCC-TESI, compared to HIO-TESI without ENCCs showed spontaneous contraction and relaxation in vitro (Movies S1–S4 in supplemental material) which was terminated in TESI that had not been supplemented with ENCCs after exposure to MB and light. This combination is known to curtail the function of ICC<sup>11,28</sup> (Movie S5 in supplemental material). However, MB does not completely inhibit contractility in HIO-TESI supplemented with ENCCs (Movies S6–S8 in supplemental material). These TESI required subsequent treatment with the neurotoxin, tetrodotoxin, to abolish movement (Movies S9–S10 in supplemental material). Our largest HIO-ENCC-TESI continued peristalsis despite administration of MB, light, and TTX (Movie S11 in supplemental material). We have had the same observation in large native segments of human and murine intestine. Future studies with higher doses of TTX may establish that increased amounts of

TTX are required for the extinction of contractility in larger or more mature constructs.

## Conclusion

Analysis of HIO-TESI implants with saline injection at the second surgery illustrated aganglionic formation of intestinal epithelium and mesenchyme without ENS. The introduction of differentiated ENCCs into developing HIO-TESI implants after 10 weeks, on the contrary, resulted in proliferative migratory cells that developed toward neuronal and glial lineages including multiple neuronal subtypes and initial measurements of ENS function.

## Declaration of conflicting interests

The author(s) declared no potential conflicts of interest with respect to the research, authorship, and/or publication of this article.

## Funding

The author(s) disclosed receipt of the following financial support for the research, authorship, and/or publication of this article: This study was funded by CIRM TRAN1-08471.

## Supplemental material

Supplemental material for this article is available online.

## References

- Amiel J, Sproat-Emison E, Garcia-Barcelo M, et al. Hirschsprung disease, associated syndromes and genetics: a review. *J Med Genet* 2008; 45: 1–14.
- Chen SH. <https://www.sages.org/wiki/hirschsprung-disease/> (accessed April 21 2017).
- Grover M, Farrugia G, Lurken MS, et al. Cellular changes in diabetic and idiopathic gastroparesis. *Gastroenterology* 2011; 140: 1575–1585.e8.
- Kraichely RE and Farrugia G. Achalasia: physiology and etiopathogenesis. *Dis Esophagus* 2006; 19(4): 213–223.
- Burns AJ and Thapar N. Neural stem cell therapies for enteric nervous system disorders. *Nat Rev Gastroenterol Hepatol* 2014; 11: 317–328.
- Schneider S, Wright CM and Heuckeroth RO. Unexpected roles for the second brain: enteric nervous system as master regulator of bowel function. *Annu Rev Physiol* 2019; 81: 235–259.
- Furness JB. Types of neurons in the enteric nervous system. *J Auton Nerv Syst* 2000; 81: 87–96.
- Furness JB. *The enteric nervous system*. Oxford: Blackwell, 2006.
- Gershon MD. *The second brain: a groundbreaking new understanding of nervous disorders of the stomach and intestine*. New York: HarperCollins, 1999.
- Finkbeiner SR, Freeman JJ, Wieck MM, et al. Generation of tissue-engineered small intestine using embryonic stem cell-derived human intestinal organoids. *Biol Open* 2015; 4: 1462–1472.

11. Schlieve CR, Fowler KL, Thornton M, et al. Neural crest cell implantation restores enteric nervous system function and alters the gastrointestinal transcriptome in human tissue-engineered small intestine. *Stem Cell Reports* 2017; 9: 883–896.
12. Fattahi F, Steinbeck JA, Kriks S, et al. Deriving human ENS lineages for cell therapy and drug discovery in Hirschsprung disease. *Nature* 2016; 531: 105–109.
13. Findlay Q, Yap KK, Bergner AJ, et al. Enteric neural progenitors are more efficient than brain-derived progenitors at generating neurons in the colon. *Am J Physiol Gastrointest Liver Physiol* 2014; 307: G741–G748.
14. Workman MJ, Mahe MM, Trisno S, et al. Engineered human pluripotent-stem-cell-derived intestinal tissues with a functional enteric nervous system. *Nat Med* 2017; 23: 49–59.
15. Chambers SM, Qi Y, Mica Y, et al. Combined small-molecule inhibition accelerates developmental timing and converts human pluripotent stem cells into nociceptors. *Nat Biotechnol* 2012; 30: 715–720.
16. Mica Y, Lee G, Chambers SM, et al. Modeling neural crest induction, melanocyte specification, and disease-related pigmentation defects in hESCs and patient-specific iPSCs. *Cell Rep* 2013; 3: 1140–1152.
17. Menendez L, Yatskievych TA, Antin PB, et al. Wnt signaling and a Smad pathway blockade direct the differentiation of human pluripotent stem cells to multipotent neural crest cells. *Proc Natl Acad Sci U S A* 2011; 108: 19240–19245.
18. Lee G, Kim H, Elkabetz Y, et al. Isolation and directed differentiation of neural crest stem cells derived from human embryonic stem cells. *Nat Biotechnol* 2007; 25: 1468–1475.
19. Hosoda K, Hammer RE, Richardson JA, et al. Targeted and natural (piebald-lethal) mutations of endothelin-B receptor gene produce megacolon associated with spotted coat color in mice. *Cell* 1994; 79: 1267–1276.
20. Laboratory TJ. Mouse strain datasheet – 021933, 2017, <https://www.jax.org/strain/021933>
21. McCracken KW, Howell JC, Wells JM, et al. Generating human intestinal tissue from pluripotent stem cells in vitro. *Nat Protoc* 2011; 6: 1920–1928.
22. Baghbaderani BA, Tian X, Neo BH, et al. cGMP-manufactured human induced pluripotent stem cells are available for pre-clinical and clinical applications. *Stem Cell Reports* 2015; 5: 647–659.
23. Boddington S, Henning TD, Sutton EJ, et al. Labeling stem cells with fluorescent dyes for non-invasive detection with optical imaging. *J Vis Exp*. Epub ahead of print 2 April 2008. DOI: 10.3791/686.
24. Barthel ER, Speer AL, Levin DE, et al. Tissue engineering of the intestine in a murine model. *J Vis Exp* 2012; 70: e4279.
25. Lee G, Chambers SM, Tomishima MJ, et al. Derivation of neural crest cells from human pluripotent stem cells. *Nat Protoc* 2010; 5: 688–701.
26. Zetzmann K, Strehl J, Geppert C, et al. Calbindin D28k-immunoreactivity in human enteric neurons. *Int J Mol Sci* 2018; 19: 194.
27. Qu ZD, Thacker M, Castelucci P, et al. Immunohistochemical analysis of neuron types in the mouse small intestine. *Cell Tissue Res* 2008; 334: 147–161.
28. Liu LW, Thuneberg L and Huizinga JD. Selective lesioning of interstitial cells of Cajal by methylene blue and light leads to loss of slow waves. *Am J Physiol* 1994; 266: G485–G496.
29. Strik C, Stommel MW, Schipper LJ, et al. Risk factors for future repeat abdominal surgery. *Langenbecks Arch Surg* 2016; 401: 829–837.
30. Boddington SE, Henning TD, Jha P, et al. Labeling human embryonic stem cell-derived cardiomyocytes with indocyanine green for noninvasive tracking with optical imaging: an FDA-compatible alternative to firefly luciferase. *Cell Transplant* 2010; 19: 55–65.
31. Sabapathy V, Mentam J, Jacob PM, et al. Noninvasive optical imaging and in vivo cell tracking of indocyanine green labeled human stem cells transplanted at superficial or in-depth tissue of SCID mice. *Stem Cells Int* 2015; 2015: 606415.
32. Watson CL, Mahe MM, Munera J, et al. An in vivo model of human small intestine using pluripotent stem cells. *Nat Med* 2014; 20: 1310–1314.